Data supplement for Fonzo et al., PTSD Psychotherapy Outcome Predicted by Brain Activation During Emotional Reactivity and Regulation. Am J Psychiatry (doi: 10.1176/appi.ajp.2017.16091072)

## Supplemental Methods

*Note: The text contained within the following sections is also reproduced in a companion publication in the same sample of participants (1): Participants and Assessments, General Inclusion and Exclusion Criteria, Behavioral Paradigms, MRI Data Acquisition, Randomization, Treatment Frequency and Length*, *Therapist Competency and Supervision in Prolonged Exposure, Treatment Structure, Post-Treatment Clinical Assessment, and Functional Image Preprocessing.*

*Participants and Assessments*

Individuals, age 18-60, were recruited via advertisement for participation in a psychotherapy treatment study for survivors of trauma. After receiving a full explanation of study procedures, participants provided written informed consent for study participation. Trained PhD-level clinicians established DSM-IV diagnoses using the Clinician-Administered PTSD Scale for PTSD (CAPS)(2) and the Structured Clinical Interview for DSM-IV Diagnosis for non-PTSD diagnoses (SCID-IV)(3). The “2 for intensity/1 for frequency” scoring rule was utilized to establish whether or not a symptom criterion was met for the establishment of diagnosis (4). IQ was estimated using the Wechsler Abbreviated Scale of Intelligence (WASI)(5). Additional secondary outcome measures included the Beck Depression Inventory-II (BDI-II)(6), a 21-item self-report inventory of depressive symptoms in which each item is rated on a 0 to 3 scale of severity. Scores range from 0 to 63. Participants provided self-report measures of PTSD symptoms using the PTSD Checklist Civilian version for DSM-IV (PCL-C)(7), a 17-item self-report measure in which PTSD symptoms are rated on a 1 to 5 scale of severity.

Total scores for this measure range from 17 to 85. Quality of life was assessed using the WHO Quality of Life BREF Scale (WHO-QoL)(8), a 26 item self-report inventory of four domains of quality of life: physical health, psychological health, social relationships, and environment. Each domain is scored on a scale ranging from 4 to 20, with higher numbers indicating better quality of life in that domain. Additionally, participants completed self-report measures of emotion regulation difficulties and style. These included the Emotion Regulation Questionnaire (ERQ)(9), a 10 item self-report measure that asks participants to rate the tendency with which they regulate and manage emotions on a 7 point Likert scale. There are two subscales, one measuring the tendency to engage in Cognitive Reappraisal and the other measuring the tendency to engage in Expressive Suppression. Scores reflect the average rating for each subscale and range from 1-7. Additionally, participants completed the Difficulties with Emotion Regulation Scale (DERS)(10), a 36 item self-report measure designed to assess multiple aspects of emotional dysregulation. Items are scored on a 5 point scale indicating the frequency with which an individual experiences a specific type of difficulty in the regulation or experience of emotion. There are six subscales: 1) Nonacceptance of Emotional Responses; 2) Difficulties Engaging in Goal-Directed Behavior; 3) Impulse Control Difficulties; 4) Lack of Emotional Awareness; 5) Limited Access to Emotion Regulation Strategies; and 6) Lack of Emotional Clarity. The score for each subscale is derived by calculating the average score for items of that subscale.

Participants with comorbid mood and anxiety disorders secondary to PTSD were included, as well as those with a history of substance dependence if abstinence had been maintained for more than three months. Regular psychotropic medication use was

permitted only for antidepressant medication (5 participants used regular selective serotonin reuptake inhibitors throughout the duration of the study) as long as the participant was stable on the same dosage, frequency, and type of medication for at least 3 months. No other regular psychotropic medications were allowed. As-needed use of benzodiazepines was allowed up to three times per week and not within 48 hours of a scan, which was verbally verified by clinician or study team member. Other types of psychotropic medications such as mood stabilizers, antipsychotics, or anticonvulsants were not permitted, nor were regular use of thyroid medications or opiates.

*General inclusion and exclusion criteria*

Inclusion criteria for all participants encompassed the following: eligibility for scanning (i.e., no metal embedded in body, not currently pregnant, no history of severe claustrophobia), good English comprehension, currently meeting criteria for a PTSD diagnosis, and intellectual function adequate for comprehension of experimenter instructions. Exclusion criteria for all participants included: lifetime diagnosis of psychosis, bipolar disorder, intellectual disability, neurodevelopmental disorders, history of neurological conditions or organic mental disorder (e.g., stroke, seizures, tumor, intracranial hemorrhage, multiple sclerosis), and substance dependence within the past three months.

*Behavioral Paradigms*

After completing baseline clinical assessment, those participants meeting eligibility criteria underwent functional magnetic resonance imaging (fMRI) on a

separate day, which occurred prior to randomization. During scan acquisition, each participant completed three separate behavioral paradigms that probe components of emotional reactivity and regulation as well as one control task. Participants also underwent a high-resolution T1 structural scan for anatomical localization of BOLD signal. All behavioral paradigms were run on a Windows XP computer, projected onto a white screen at the base of the scanner bed, viewed by the participant using a mirror mounted above the head coil, and responded to via keypress of a customized MRI-safe button box.

Emotional Reactivity Task: This previously-published paradigm (11) probes goal-irrelevant emotional reactivity via conscious and non-conscious (backwardly masked) presentation of fearful and neutral face stimuli. Faces were black and white photographs drawn from a standardized series developed by Ekman & Friesen (12), displayed in an elliptical shape that eliminated background and hair, and then artificially colorized in red, yellow, or blue and equalized for luminosity. Participants were instructed to identify, as quickly as possible, the color of the face via keypress of a button box. Importantly, identification or processing of the facial affect was only incidental and not the focus of the task. Faces displayed either fearful or neutral facial expressions and were presented in a conscious and non-conscious format. Each trial lasted 2000 ms and began with presentation of a fixation cross to cue attention to the screen center (200ms) followed by a 400 ms latency period. Faces were then presented for 200ms, and participants were given 1200ms to respond with the color of the face presentation. For conscious presentation trials, one face (fearful or neutral) was presented for the entire 200ms. For

the non-conscious masked fear condition, a fearful face was presented for 16.67 ms and then immediately backwards masked with a neutral face (in the same color tint and of the same gender, but with a different identity) for the remainder of the 200ms face presentation period (183.33ms). For the non-conscious masked neutral condition, the same backwards-masking procedure was utilized, but the initial quick prime was also a face with a neutral expression from a different individual than the masked face. Faces were presented in 16 blocks across one task run, with face color and gender randomized across blocks. Each block consisted of 10 face presentations of a particular emotion type and masked or unmasked. Four blocks of each emotion (fear or neutral) and masking combination (masked or unmasked) were presented in a counterbalanced format, resulting in 16 blocks total. Stimuli were presented using Presentation software on a computer running Windows XP. Following completion of the color identification task while undergoing scanning, participants completed a forced-choice test (whether or not they saw a fearful face on each trial) using the same stimuli under the same conditions as the scanning procedure in order to assess adequacy of the masking procedure. This entire task lasted 9 minutes and 36 seconds.

Emotional Conflict Task: This well-characterized paradigm (13, 14) assesses both emotional conflict and emotional conflict regulation, an implicit regulatory process in which the behavioral interference due to incongruent emotional stimuli is automatically suppressed from conflict trial to conflict trial. On each trial, participants were presented with an emotional face and instructed to identify the underlying facial emotion (fearful or happy) while ignoring an overlying emotion distractor (emotion word - “FEAR” or

“HAPPY”) as quickly and accurately as possible. Trials varied such that emotional distractor words were either congruent or incongruent with the underlying facial expression. Each task consisted of 148 presentations of facial photographs drawn from a set by Ekman & Friesen (12). Stimuli were presented for 1000 milliseconds (ms) in a fast event-related design with a varying inter-stimulus interval of 3000-5000 ms in a pseudo-randomized order counterbalanced for facial expression, gender, word, and response button. All participants of the study went through a practice version prior to entering the scanner to make sure proficiency (minimum 80% accuracy) was reached and the task instructions were understood. The entire task lasted 13 minutes and 14 seconds.

Gender Conflict Task: This task was developed as a comparator paradigm to isolate emotion-specific effects within a conflict context (15). Participants viewed the same black and white facial stimuli with fearful and happy expressions as in the emotional conflict task, but in this task the goal was to identify face gender and ignore a congruent or incongruent overlaid gender word (“MALE” or “FEMALE”). Task characteristics were analogous to the emotional conflict task, with the exception of task instructions and distractor stimuli. This task also lasted 13 minutes and 14 seconds.

Reappraisal Task: This emotion regulation task utilized here is described in a prior publication (16). In brief, the task consisted of presentation of 30 negative and 15 neutral photographs taken from the International Affective Picture System (IAPS) database. Each trial consisted of a 2 second cue presentation (“Look” or “Decrease”),

then a 7 second photo presentation, then a 4 second period to rate their level of emotional negativity at that moment using button box key press on a scale ranging from 1 (Not at all negative) to 5 (Very much negative). The scale was presented visually to participants during this period. There was then a 1 to 3 second rest period before the next cue presentation. Photographs were presented in a pseudorandom order such that no more than 2 of the same instruction (“Look” or “Decrease”) could be presented consecutively, and no more than 4 negative stimuli could be presented consecutively. Fifteen negative photographs were presented with a cue to “Look” and 15 were presented with a cue to “Decrease”, while all neutral photos were presented with a “Look” cue. Negative photographs depicted illness and/or injury (21 photos), acts of aggression (3 photos), members of hate groups (2 photos), transportation accidents (2 photos), and bodily waste (2 photos). Neutral photographs portrayed inanimate objects (10 photos) or neutral scenes (5 photos). Prior to undergoing the task, participants were instructed that, when cued to “Look”, they were to focus attention on the photo and allow their emotional reaction to occur naturally. When cued to “Decrease”, participants were instructed to attempt to reduce their emotional reaction to the photo by thinking of something that makes the photograph seem less negative to them (i.e. cognitive reappraisal). Participants were given practice examples of photographs and cognitive reappraisal strategies prior to entering the scanner, and they were also given the opportunity to practice reappraisal using their own spontaneously generated thought strategies on negative IAPS pictures (not utilized during scanning). The entire task lasted 11 minutes 28 seconds. The contrasts of interest were looking at a negative picture vs. looking at a neutral picture (Look Negative vs. Look Neutral) and using

cognitive reappraisal to decrease negative emotion to a negative picture vs. looking at a negative picture (Decrease Negative vs. Look Negative).

*MRI Data Acquisition*

Images were acquired on a 3-T GE Signa scanner using a custom-build head coil. During performance of each task, twenty-nine slices (4.0 mm thickness, 0.5 mm gap) were acquired in the axial direction across the whole brain using a T2*-weighted gradient echo spiral pulse sequence (TR = 2000 ms, TE = 30 ms, flip angle = 80°, 1 interleaf, field of view = 22 cm, 64x64 matrix). A high-resolution T1-weighted image (three-dimensional inversion recovery spoiled gradient-recalled acquisition in the coronal place with the following parameters: inversion time = 300 ms, TR = 8 ms, TE = 3.6 ms, flip angle = 15°, field of view = 22 cm, 124 slices, matrix = 256x192, number of excitations = 2, acquired resolution = 1.5 x 0.9 x 1.1 mm) was likewise obtained for each participant. During behavioral paradigms, measures of heart rate and respiration were collected and used to remove physiological noise from the time series (17).

*Randomization*

Following completion of baseline clinical assessments and fMRI scan, participants were randomized to one of two arms: 1) Immediate treatment with prolonged exposure therapy; or 2) Treatment waitlist. This occurred using random selection of a number from the string of digits 1 to 10, within an even selection indicating assignment to immediate treatment and an odd selection indicating assignment to waitlist. A total of sixty-six (N=66) individuals were randomized, with 36 being

randomized to immediate treatment, and 30 to treatment waitlist. If randomized to immediate treatment, participants commenced treatment with a clinical psychologist trained to deliver prolonged exposure therapy. If randomized to waitlist, individuals were instructed they would have a 10-week waiting period after which they would undergo a second clinical assessment and fMRI scanning session. After completion of this second assessment, individuals on treatment waitlist were then assigned to a study therapist for completion of prolonged exposure therapy, which was provided for ethical reasons and not for neuroimaging analyses (since this would be outside of the randomized trial context).

*Concurrent TMS-fMRI causal mapping*

As an additional causal measure to establish predictive brain circuitry, a random subset of individuals randomized to immediate treatment were invited to undergo a concurrent TMS-fMRI scanning session conducted according to established protocols (18). On average, this session occurred about two weeks following the task-based fMRI session. In brief, the high resolution anatomical image collected at the baseline task scanning session was calibrated with skin and scalp for individualized site targeting using a Polaris Vicra camera with Brainsight neuronavigation software (Rogue Research, Montreal Canada). Participants wore a lycra swimcap to facilitate marking of stimulation sites. Motor threshold (MT) was defined as the lowest possible stimulation intensity at a site that induced a consistent visible response in the contralateral abductor pollicis brevis (thumb) muscle, a common within-subject metric for individualization of TMS intensity. Given existing evidence for some efficacy of repetitive TMS treatment

(particularly delivered to the right dorsolateral prefrontal cortex) in alleviating PTSD symptoms (19), we focused stimulation on two sites in the right dorsolateral prefrontal cortex: the right anterior middle frontal gyrus (aMFG; part of the resting state salience network), and the right posterior middle frontal gyrus (pMFG; part of the resting state executive control network). The primary site of interest was the right pMFG, given prior TMS treatment studies that have used the “5cm anterior to the motor cortex” localization rule and demonstrated significant effects on PTSD symptoms (20); the pMFG falls closely within this demarcation. The aMFG was utilized as an active comparison site to control for the subjective experience and peripheral nerve effects of TMS stimulation. Stimulation sites were derived from an independent components analysis (ICA) of resting-state fMRI data in an independent sample of 38 healthy participants (18). Before the concurrent TMS-fMRI scan, the ICA map was warped to the participant’s native brain space using the inverse of the normalization matrix, and this overlay was utilized to derive individualized sites for targeting using frameless stereotactic neuronavigation with Brainsight software (Rogue Research, Montreal Canada). Once sites were marked, participants underwent scanning using parameters sensitive to BOLD signal contrast: T2*-weighted, oblique (axial to anatomy) slices of the full brain (31 slices, 4.0 mm thick, 0.5 mm gap) sampled via a T2* weighted gradient echo spiral pulse sequence (TR=2000, TE=30, flip angle=85 deg, 1 interleave, FOV=22 cm, 64x64 matrix) and using a 400 ms gap between volumes for TMS single pulse delivery. TMS was delivered via a MagVenture MR-compatible MRI-B91 figure-eight TMS coil held in place by a custom-built MRI coil holder, triggered by a MagVenture X100 stimulator located outside the room and connected to the coil via the penetration panel. The TMS sites were

repositioned for each participant by sliding the participant out of the magnet bore, adjusting the coil position, and returning the participant into the bore. Stimulation intensity was individually determined and corresponded to 120% of resting MT. At each site, 70 TMS pulses were delivered over 5 minutes (147 volumes) in a block design with 7 pulses per block (16.8 sec TMS “on” periods with 16.8 sec TMS “off” periods between blocks) and 10 blocks per run. Pulses were delivered between collections of functional volumes to avoid corruption of BOLD signal. In total, 17 of 36 individuals in the immediate treatment arm underwent TMS-fMRI stimulation and completed both sites of stimulation.

*Treatment Frequency and Length*

Treatment sessions occurred on either a once or twice-weekly basis, for a total of either 9 or 12 90-minute sessions, according to manualized procedures (21). We chose to utilize a flexible treatment frequency format and allow for either once or twice-weekly sessions in order to reduce participant burden and minimally disrupt the participants’ existing scheduled commitments. The variable duration of treatment (9 or 12 sessions) was utilized in order to ensure that each participant received the maximal therapeutic benefit from prolonged exposure while also allowing for inter-individual differences in rate of therapeutic responses, which has been previously employed in similar treatment outcome designs (22). We note that allowing for this heterogeneity in treatment delivery could introduce other sources of variation that might impact response to the intervention. We examined this possibility post-hoc (see Supplemental Results), but it

should be noted that these analyses are likely underpowered to detect such effects, if present.

At sessions 2, 4, 6, and 8 individuals were administered the PTSD-Checklist Civilian Version for DSM-IV (PCL-C)(7) as well as the Beck Depression Inventory-II (BDI-II)(6) to track response to treatment. The benchmark used to establish adequacy of treatment response at Session 9 and subsequent termination was a reduction in Session 8 PCL-C scores to less than 30% of the PCL-C total score at intake (i.e. 70% reduction from baseline)(22). If individuals met this benchmark, they were given the option to discontinue treatment after Session 9. If individuals did not meet this benchmark and/or wished to continue for an additional 3 sessions, treatment was terminated after Session 12. If treatment continued to 12 sessions, PCL and BDI measures were administered at Sessions 10 and 12.

*Therapist Competency and Supervision in Prolonged Exposure*

All psychologists received training in delivery of prolonged exposure and were deemed to meet competence in delivery of the treatment by one of the treatment developers, consultant to the study, and clinician supervisor Barbara Rothbaum, Ph.D. Dr. Rothbaum provided weekly group supervision to study therapists and reviewed video recordings of treatment sessions to rate compliance with the treatment protocol and to provide supervision. Dr. Rothbaum watched the entirety of the first three treatment sessions for each therapist to ensure therapist familiarity and competence with all major components of the treatment (all delivered in the first three sessions), and she continued to review relevant portions of remaining sessions as directed by study

therapists. All study therapists demonstrated good compliance with the therapy protocol and with no significant deviations, as demonstrated by good-to-excellent supervisor ratings of treatment session adherence.

*Treatment Structure*

Prolonged exposure therapy was delivered according to manualized procedures (21). All sessions were audio recorded on a digital voice recorder (entrusted to the participant to take home with them and for use in completing imaginal exposure homework assignments) as well as a digital video recorder (for the purposes of assessing treatment adherence, therapist competency, and clinical supervision). In brief, the structure and progression of treatment is as follows. Session 1 consisted of psychoeducation on posttraumatic stress disorder symptoms, the rationale for treatment, and treatment structure. It also involved additional assessment by the therapist of trauma history (including the index trauma, already established at intake), current symptoms, and current impairment. Breathing retraining was taught at the end of Session 1 and practiced collaboratively in session, which consisted of a normal inhalation and a controlled and slow exhalation with internal repetition of a calming word or phrase (e.g., “Calm”) and a pause between exhalation and next inhalation, which was audiotaped for the participant. Session 2 consisted of homework review, self-report measures, a discussion of common reactions to trauma, a rationale for exposure as a treatment tool, construction of an exposure hierarchy for *in-vivo* exposure exercises, and selection of 2 to 3 hierarchy items for homework practice. Session 3 involved homework review, a brief rationale for imaginal exposure, and the first imaginal

exposure in session for 45-60 minutes. This was followed by a processing portion in which the therapist and participant discussed the participant's experience of the exposure, any insights received through that process, and areas to be further addressed in future exposures. Homework was then assigned (including completion of in-vivo exposures and imaginal exposures daily and practice of breathing retraining). Session 4 consisted of the same format as Session 3 but without the discussion of rationale for imaginal exposure.

Beginning in Session 5, the concept of trauma memory "hotspots" was discussed with participants, which were points in the memory during which the participant experienced the highest level of distress. The in-session imaginal exposure began to shift towards emphasizing hotspots in the memory in Session 5, at earliest, and sometimes Session 6 if agreed to be clinically appropriate by the participant and therapist. Sessions 6, 7, and 8 involved a similar format, with homework review, imaginal exposure to hot spots, processing, and homework assignment. For participants reaching the PCL clinical benchmark in Session 8, and agreeing to end in 9 sessions, Session 9 consisted of homework review, a brief imaginal exposure of the entire trauma memory conducted in-session (20-30 minutes), a brief processing, and a final review of treatment progress and skills acquired. For participants not reaching the clinical benchmark and/or wishing to continue for an additional 3 sessions, Sessions 9-11 maintained the same format as Sessions 4-8. In this case, Session 12 served as the final session (which assumed the aforementioned format).

*Post-Treatment Clinical Assessment*

Approximately 4 weeks following the final treatment session, participants completed a post-treatment clinical assessment and repeated the imaging protocol. A 4-week period was chosen to intercede between final session and post-treatment assessment in order to allow treatment changes to consolidate and symptom levels to equilibrate and to not overlap with the treatment period in assessing PTSD symptoms past month. Moreover, brain changes from baseline noted at this time delay will be more representative of those changes conveying long-term therapeutic improvements. Participants were administered the CAPS and SCID again at post-treatment to assess change in PTSD symptoms and comorbid diagnoses.

*Functional Image Preprocessing*

Data were preprocessed using FSL tools (23). Affine transformation of functional to structural images using boundary-based registration based upon tissue segmentation as implemented in FSL's FLIRT was added to non-linear normalization of each participant's T1 image to the Montreal Neurological Institute (MNI) 152-person 1 $mm^3$ T1 template using FNIRT from FSL 5.0 (24). Functional images were subsequently aligned to the middle volume of the run. Global signal corresponding to segmented white matter and CSF was regressed out of motion-corrected functional images, which were isotropically smoothed with a 6 mm full-width half max (FWHM) to account for individual anatomical variability. Participants with a root mean square absolute movement > 3mm across the mean of the squared maximum displacements in each of

the 6 estimated translational and rotational motion parameters for each functional run were excluded from further analysis for quality control purposes. This amounted to 3 participants for the Emotional Reactivity task (2 in immediate treatment, 1 in waitlist), 3 participants for the Emotional Conflict Task (1 in immediate treatment, 2 in waitlist), 3 participants for the Gender Conflict Task (2 in immediate treatment, 1 in waitlist), and 5 for the Reappraisal Task (3 in immediate treatment, 2 in waitlist). Thus, the final utilized sample size for each analysis were: N=63 for the Emotional Reactivity Task, the Emotional Conflict Task, and the Gender Conflict Task; N=61 for the Reappraisal Task; and N=17 for the TMS/fMRI analysis.

*Individual-Level Analysis of Functional Images*

For each participant, time point, and task paradigm, regressors modeling trials of interest were convolved with the hemodynamic response function. For concurrent TMS-fMRI, the regressor of interested corresponded to “TMS on” blocks for the right pMFG and right aMFG, and the contrast of right pMFG vs. aMFG stimulation served as the contrast of interest. First-level GLMs were conducted in SPM 8.0 (25) using relevant HRF-convolved regressors along with six parameters corresponding to nuisance regressors for within-session motion.

For the Emotional Reactivity task, regressors corresponded to the onset of facial stimuli for four conditions of interest: conscious fear, conscious neutral, non-conscious fear, and non-conscious neutral. The *a priori* contrasts of interest were the differences in activation for conscious fear vs. neutral and for non-conscious (masked) fear vs. neutral, each allowing for the isolation of fear reactivity processes within a particular

processing depth. As there was no non-facial comparator experimental condition included in this paradigm that could be used to examine activation magnitudes for each face type specifically, e.g., a scrambled face or shape processing condition, we note that this task's capacity for dissociating responses to fearful and neutral faces separately is limited. We therefore focused only on the assessment of within-subject contrast magnitudes (fearful minus neutral) for each processing depth (conscious or non-conscious), consistent with prior investigations utilizing this paradigm (11). Additionally, this contrast achieves the best experimental control, as it eliminates confounds including procedural aspects of the task and perception of facial features in general.

For the Emotional Conflict task, regressors corresponded to the onset of stimuli defined by face valence (Fear or Happy), congruency (Incongruent or Congruent), and prior trial type (Post-incongruent or Post-congruent) in order to model conflict regulation effects. This resulted in 8 different trial types in total, along with nuisance regressors for error trials and post-error trials (when applicable). The *a priori* contrasts of interest were Incongruent vs. Congruent trials (conflict), Post-incongruent Incongruent trials vs. Post-congruent Incongruent trials (iI vs. cI; an established measure of conflict regulation), and Congruent Fear vs. Congruent Happy trials, an additional probe of emotional reactivity to assess generalizability of effects from the Emotional Reactivity Task.

For the Gender Conflict task, regressors corresponded to onset of face stimuli defined by congruency and prior trial type, resulting in four stimulus types total, along with nuisance regressors for error and post-error trials. The *a priori* contrasts of interest

here were Incongruent vs. Congruent (conflict) and Post-incongruent Incongruent vs. Post-congruent Incongruent (conflict regulation).

For the Reappraisal paradigm, regressors for the Look Neutral, Look Negative, and Reappraise Negative conditions were modeled from onset to offset of the picture stimulus to capture regulatory and reactivity processes. The *a priori* contrasts of interest here were Look Negative vs. Look Neutral, a measure of emotional reactivity to complex affective pictures, and Reappraise Negative vs. Look Negative, a measure of cognitive reappraisal-related emotional regulatory activity which controls for picture valence and arousal-related processes.

*Assessing Treatment Moderation Effects of Clinical Variables, Demographics, and Task Behavior*

To assess baseline behavioral, clinical, and demographic characteristics for moderation of treatment response, generalized linear mixed models with a robust estimator were implemented in SPSS 21.0 (26). We utilized a random intercept and fixed effects of time, treatment arm x time, moderator variable, time x moderator variable, and arm x time x moderator variable. Continuous moderator variables were mean-centered and categorical moderator variables (such as gender) were effects coded, while treatment arm was also effects-coded. Analyses employed a full intent-to-treat framework with inclusion of the entire randomized sample and all post-assessment data available, with no artificial imputation of missing data.

*Identifying Task-Related Activation*

To identify task-related activation patterns across participants at baseline (i.e. unrelated to psychotherapy), individual subject contrast images for each task condition of interest were analyzed using threshold free cluster enhancement in FSL with a sign-flip permutation test (27). The distribution of effects was computed over 5,000 permutations per positive and negative side of the tail for each contrast, i.e. task effect. The significance threshold was set at a family-wise error corrected $p < 0.05$ (two-tailed). Task effects were assessed in both a whole brain exploratory analysis as well as within an anatomically constrained region of interest mask specifying *a priori* brain structures relevant to PTSD and psychotherapy effects (Figure S1). This mask included the bilateral amygdala (derived from subcortical surface models implemented in FSL's subcortical segmentation program FIRST(28)), bilateral anterior insula (derived from the Automatic Anatomical Labeling (AAL) atlas (29), with the anterior portion defined as $y > 0$), anterior and mid-cingulate cortex ranging from the subgenual portion at its point adjoining the ventral striatum all the way up to dorsal anterior and mid-cingulate cortex (derived from the anterior cingulate, mid-cingulate, and olfactory cortex sites of the AAL atlas with $y > 0$, $-14 < x < 14$, and $-12 < z < 44$), and bilateral lateral and dorsolateral prefrontal cortex (defined as the bilateral inferior frontal, middle frontal, and superior frontal gyri from the AAL atlas constrained by $z > -4$, $16 < x < 60$ for right hemisphere, $-60 < x < -16$ for left hemisphere, and $y > -10$). Whole brain analyses were restricted to a probabilistic gray matter mask (> 40%) derived from an independent sample of healthy participants.

*Assessing Treatment Moderation Effects of Brain Function*

To identify functional brain characteristics moderating responses to prolonged exposure therapy (as assessed by our primary outcome measure—total scores from the Clinician Administered PTSD Scale for DSM-IV at pre- and post-treatment), we employed the MacArthur approach (30) embedded in our longitudinal linear mixed effects models. Moderation effects were assessed on a voxel-wise level using linear mixed models (nlme package)(31) implemented in R (32). Briefly, for each contrast of interest, each voxel within an independently defined whole brain gray matter mask from participant baseline images was used to predict CAPS total scores in interaction with treatment and time effects using restricted maximum likelihood (ReML) estimation. We specified a random intercept and mean-centered (for the continuous moderator) or effects-coded (for treatment arm) fixed effects of time, time x treatment arm, baseline activation, time x baseline activation, and the time x treatment arm x baseline activation interaction. This latter three-way interaction effect specifies the moderation of the time x treatment arm interaction effect, i.e. differential change across time in PTSD symptoms between groups, as a function of baseline brain activation. To control for Type I error inflation, F-statistics for the omnibus three-way interaction moderation effect were then subjected to voxel-level false discovery rate (FDR) correction ($q < 0.05$) within a region of interest mask specifying *a priori* brain structures relevant to PTSD and psychotherapy effects. Voxels surviving the $q < 0.05$ FDR corrections were then clustered for the purposes of extraction, visualization, and verification using IBM SPSS 21.0. Generalized linear mixed models with a robust estimator were utilized to confirm significance of voxel-wise results.

*Assessing Predictive Value of Brain Moderators for Remission from PTSD*

In order to characterize how well brain activation moderators identified with the voxelwise analyses are able to predict remission status at the end of treatment, additional analyses were undertaken using average individual-level activation values from task-based activation clusters that moderated the effect of treatment. In order to predict remission and allow for uniform comparisons across models, these analyses were restricted to treatment/waitlist completers who had high-quality imaging data (i.e., not excluded due to excessive movement or missing data) for all of the tasks (22 in treatment and 22 in waitlist). First, individuals were classified as diagnostic remitters or non-remitters according to a widely utilized clinical research criterion of post-treatment CAPS total score less than or equal to 20. We then used a linear discriminant analysis implemented in IBM SPSS 21.0 (26) to classify remission from PTSD using the predictors of group assignment (treatment or waitlist) and baseline PTSD severity (CAPS total scores). We then created a variable specifying whether, for each subject, the discriminant function correctly classified him or her as reaching remission or not. Then, to assess the incremental validity of brain activation moderators in predicting remission, we ran another linear discriminant analysis with predictors for group, baseline PTSD severity, and average activation values for each cluster identified in the voxelwise moderation analysis (separate models were used for clusters from *a-priori* region of interest-restricted analyses and those from whole-brain analyses). Another variable was then created specifying whether, for each subject, the discriminant function correctly classified him or her as reaching remission or not. McNemar's test with the

Agresti-Coull correction (33) was then utilized to compare the distributions of these two classification accuracy variables in order to ascertain whether or not the addition of brain activation values resulted in significantly better predictive accuracy. In addition, for each discriminant analysis a leave one out cross-validation procedure was utilized to determine the predictive accuracy of the model in properly assigning the participant left out at each stage to the correct remission status. In order to assess sensitivity and specificity of brain activation moderators in predicting remission status at end of treatment, receiver-operator curves were constructed using average individual subject activation values for each cluster identified in the voxelwise moderation analysis. These curves were then plotted, and the combination of sensitivity and 1-specificity values that showed maximal differentiation from the diagonal were identified (see Tables S2 and S3).

*Exploratory Analyses: Assessing the Functional Significance of Treatment-Moderating Activation*

In order to support the reader in interpreting the functional significance of the treatment-moderating activation effects detected in the voxel-level analyses, we conducted exploratory analyses to relate treatment-moderating activation at baseline to various self-report and behavioral measures. Given the hypotheses and conceptual framework for the study, we focused specifically on self-report measures of emotion regulation style (ERQ), and difficulties (DERS), as well as average trial-by-trial distress ratings during the reappraisal paradigm for experiencing the affect from a negative picture (Look Negative vs. Look Neutral) and regulating the affect from a negative

picture (Reappraise Negative vs. Look Negative). Average activation was extracted from clusters showing significant group-level treatment-moderation effects in the region of interest-constrained analyses, and non-parametric correlations (Spearman's rho) were computed in IBM SPSS 21.0 (26) to assess the relationship between average activation and these measures of emotion regulation and emotional reactivity across the entire sample at baseline. Since these were undertaken as exploratory analyses, we report significant relationships at $p < 0.05$ uncorrected for multiple comparisons.

## Supplemental Results

*Sample Characteristics*

See CONSORT chart (Figure S2) for complete details of participant recruitment, enrollment, and retention, and Tables 1 and 2 in the main text for detailed information on sample characteristics and outcome data. The final randomized sample included 66 individuals, with 36 being randomized to immediate treatment and 30 randomized to waitlist. Of those randomized, 25 completed the post-treatment clinical assessment in the immediate treatment group, and 26 randomized to waitlist completed the post waitlist clinical assessment. Though there were a higher number of dropouts in the immediate treatment group, the difference in frequency of dropouts between groups was not statistically significant (two-tailed Fisher's exact test $p = 0.141$). Across groups, participants did not differ on age, education, PTSD symptom severity, verbal IQ, performance IQ, or full scale IQ. Comorbid major depression was equally represented in the immediate treatment and waitlist groups (50% in immediate treatment group, 56.67% in waitlist group; two-tailed Fisher's exact test $p = 0.628$), as was use of SSRI/SNRI medications (two-tailed Fisher's exact test $p = 1.00$, N=3 participants in treatment arm, N=2 participants in waitlist). In those individuals randomized to immediate treatment, 2 participants were taking an SSRI, and 1 participant was taking an SSRI and a benzodiazepine (with no usage 48 hrs. before a study appointment). In those individuals randomized to waitlist, 2 individuals were taking an SSRI, and there were no individuals taking a benzodiazepine (either alone or in combination with an SSRI). Thus, the groups were well matched on all relevant clinical and demographic variables. At the end of treatment/waitlist, none of the participants randomized to waitlist

reached the remission criterion (defined as post-treatment CAPS total score less than or equal to 20). In those randomized to prolonged exposure treatment, however, 10 participants reached remission from PTSD while 15 participants did not.

*Timeline of Participant Scans*

After undergoing baseline clinical assessments and being enrolled into the study, participants completed their pre-treatment task-based fMRI scan. Of those participants randomized to immediate treatment, a random subset underwent simultaneous TMS/fMRI. This occurred, on average, about two weeks following the pre-treatment task-based fMRI scan session ($M$ = 16.3 days, $SD$ = 8.7 days). After the TMS/fMRI scan, individuals had their first session of prolonged exposure about two weeks later ($M$ = 13.9 days, $SD$ = 10.5 days). Across the entire treatment-randomized group, individuals attended their first session of prolonged exposure about one month after the pre-treatment task-based fMRI session ($M$ = 29.9 days, $SD$ = 10.9 days). Within the treatment-randomized group, the average length of time from the pre-treatment fMRI session to the post-treatment fMRI session was about 13 weeks ($M$ = 90.1 days, $SD$ = 22.67 days), and the average length of time from the final treatment session to the post-treatment scan was about 4 weeks ($M$ = 28.67 days, $SD$ = 8.50 days). Within the waitlist-randomized group, the average length of time from the pre-waitlist fMRI session to the post-waitlist fMRI session was about 11 weeks ($M$ = 81.1 days, $SD$ = 9.3 days). Though the average length of time between pre and post scan sessions was slightly longer for treatment-randomized individuals, this difference was not significant ($t$ = 1.793, $p$ = 0.083).

*Assessing the Impact of Treatment Frequency and Duration on Symptom Change*

Of those individuals randomized to immediate treatment (N=36), 22 individuals underwent treatment once a week, and 14 individuals underwent treatment twice a week. In order to ascertain if these individuals systematically differed in important characteristics, we compared baseline demographic and symptom profiles between those individuals selecting to undergo treatment at different frequencies. These individuals did not differ in terms of demographics (age, education, gender), presence of comorbid major depression, or baseline PTSD symptoms (all *p's* > 0.15). We also examined self-reported quality of life (WHO Quality of Life scale) across several domains, as different environmental characteristics (i.e. owning a car, having intact social relationships, being employed, etc.) could feasibly influence both quality of life and decision regarding treatment frequency. None of the domains of the WHO-Quality of Life Scale (physical, environmental, social, psychological, overall) significantly differed between individuals undergoing treatment at different frequencies (all *p's* < 0.12). We used linear mixed models in an intent-to-treat framework to examine the effect of treatment frequency on symptoms reductions. The frequency of treatment did not moderate the effect of treatment in the group randomized to prolonged exposure (Time x Treatment Frequency interaction $F = 0.53$, $p = 0.43$), and the effect of treatment on CAPS total scores was still highly significant when controlling for treatment frequency ($F = 88.38$, $p < 0.001$).

Next, we examined the effect of treatment duration (9 vs. 12 sessions) on the reported results. Of treatment completers (24 of 36 participants in those randomized to

immediate treatment), 16 completed 12 sessions of prolonged exposure. Number of sessions completed did not relate to age, education, gender, or baseline PTSD symptoms (all *p's* > 0.25), nor did number of sessions completed relate to any domains of quality of life (all *p's* > 0.36). We next examined whether number of sessions completed influenced treatment outcomes. Using a linear mixed model in an intent-to-treat framework and examining treatment duration as a moderator of symptom reduction in the immediate treatment group, we observed that number of sessions of treatment completed did not moderate the effect of treatment on CAPS symptoms (Time x Treatment Duration $F = 0.20$, $p = 0.66$), and the effect of treatment was still significant when controlling for duration of treatment ($F = 6.49$, $p = 0.01$). These results are consistent with the primary intent-to-treat analysis, which demonstrate that prolonged exposure was effective at reducing PTSD symptoms in an intent-to-treat framework.

*Task Behavior*

At baseline, there were no significant differences in task behavior between groups across any paradigm assessed (all *p's* > 0.09). Of the behavioral metrics collected, there were no significant relationships with PTSD symptom severity (CAPS total scores) for any behavioral paradigm. Examining relationships in behavior across paradigms, higher ratings of distress following Decrease Negative trials on the reappraisal paradigm were associated with longer RTs for color identification on all trials of the emotional reactivity task (all rho's > 0.31, all *p's* < 0.015). This effect was non-specific for emotion type and masking, and it was not present for the other conditions of

the reappraisal task. There were no other significant cross-task behavioral relationships observed.

*Demographic/Clinical Variable Moderation*

Neither age, years of education, full scale IQ, verbal IQ, performance IQ, nor presence of comorbid major depression moderated treatment response to prolonged exposure (all $p$'s > 0.20). Sustained use of antidepressant medication throughout the study did not significantly moderate the group x time interaction ($F$ = 1.51, $p$ = 0.23).

*Task Behavior Moderation*

Reaction times on all trial types of the emotional reactivity task displayed significant interactions with group x time effects on CAPS total scores (all $p$'s < 0.045), though in each case these effects were due to interactions with symptom change over time not in the treatment group (all $p$'s > 0.21) but in the patient waitlist group only (all $p$'s < 0.027), with those individuals displaying quicker reaction times to color identification and randomized to waitlist displaying larger reductions in symptoms at post-waitlist assessment (estimated mean difference of about 10-15 points on CAPS total scores). None of the other task behavioral indices displayed significant moderation effects.

*Baseline Task Activation*

Emotional Reactivity Task

During conscious processing of fearful vs. neutral faces, the region of interest-constrained analysis revealed activation of the right middle frontal gyrus/inferior frontal gyrus, right anterior insula, and the middle cingulate cortex. No significant deactivations were detected for this contrast. In the whole brain exploratory analysis, additional activations were detected in the right precuneus/superior parietal lobule, brainstem, and right mid-orbital gyrus. No significant deactivations were detected in the whole brain analysis.

During nonconscious processing of masked fearful vs. masked neutral faces, the region of interest-constrained analysis revealed activation of the left superior frontal gyrus, the right inferior frontal gyrus, and the right amygdala. No deactivations were detected. The whole brain analysis revealed additional activation of the brainstem, and deactivation was observed in the right hippocampus, right middle temporal gyrus, and right putamen.

Emotional Conflict Task

For the incongruent vs. congruent trial contrast, the region of interest-constrained analysis identified activation in the bilateral anterior insula, the left inferior frontal gyrus, and left superior frontal gyrus. No areas of deactivation were observed. In the whole brain exploratory analysis, large clusters of activation were detected in both hemispheres, extending from the temporal pole through the insula, putamen, inferior frontal gyrus, middle frontal gyrus, superior frontal gyrus, and precentral gyrus, with the

cluster in the left hemisphere continuing to extend into the medial frontal gyrus and middle cingulate cortex. Additional areas of activation observed included the left inferior parietal lobule/supramarginal gyrus/angular gyrus, bilateral middle cingulate cortex, left middle temporal gyrus, midbrain, right precentral gyrus, and right inferior parietal lobule. No areas of deactivation were detected in the whole brain analysis.

In the congruent fear vs. congruent happy contrast, the region of interest-constrained analysis detected activation in the left inferior frontal gyrus. No clusters of deactivation were observed. In the whole brain analysis, additional activation was observed in the right middle temporal gyrus, and deactivation was observed in the left hippocampus.

In the conflict regulation contrast (post-incongruent incongruent vs. post-congruent incongruent trials), the region of interest-constrained analysis revealed activation of the pregenual anterior cingulate cortex and deactivation of the bilateral inferior frontal gyrus/middle frontal gyrus/superior frontal gyrus and middle cingulate cortex. The exploratory whole brain analysis revealed no additional activations, but it identified very large clusters of deactivation spanning multiple regions of the dorsolateral and dorsomedial prefrontal cortex as well as lateral and medial parietal cortex.

Reappraisal Task

The region of interest-constrained analysis of the Look Negative vs. Look Neutral contrast revealed activation of the right middle frontal gyrus, left anterior insula, left dorsal anterior cingulate, and the left amygdala. There were no areas of deactivation

observed. The whole brain exploratory analysis yielded additional activation in the bilateral cuneus, left middle occipital gyrus, and right inferior occipital gyrus/fusiform gyrus, and deactivation was observed in the left lingual gyrus and left postcentral gyrus.

The region of interest-constrained analysis of the Reappraise Negative vs. Look Negative contrast yielded activation of the right inferior and middle frontal gyri (P. Opercularis and P. Triangularis), the left middle and superior frontal gyri, and the right anterior insula. There were no areas of deactivation observed. The whole brain exploratory analysis yielded additional extended activation in large posterior portions of both hemispheres, including visual cortex, inferior and lateral temporal cortex, and precuneus, as well as the bilateral supplementary motor area and motor cortex.

*Baseline Functional Brain Moderators: Exploratory Whole Brain Analyses*

Emotional Reactivity Task

An exploratory whole-brain analyses yielded additional moderation effects for conscious fear vs. neutral. In all of the following brain regions, whole-brain moderation effects were driven by greater baseline brain activation in the immediate treatment group predicting greater differential symptom reductions: left posterior superior temporal cortex, left anterior cingulate/mid-cingulate/superior medial gyrus, left inferior temporal gyrus, right middle frontal gyrus, left inferior frontal gyrus (P. Triangularis), left superior frontal gyrus, left angular gyrus, right anterior cingulate, left middle frontal gyrus, and right cerebellum (all $p$'s < 0.003). In the left middle temporal gyrus, the moderation effect was driven by less baseline brain activation to conscious fear vs. neutral in the

immediate treatment group group predicting greater differential symptom reductions ($p < 0.003$). No effects were detected for nonconscious (masked) fear vs. neutral.

Emotional Conflict Task

No significant moderation effects were detected in the whole brain exploratory analysis for conflict, conflict regulation, or emotional reactivity (congruent fear vs. happy).

Reappraisal Task

No significant moderation effects were detected in the whole brain analysis for either contrast of the reappraisal task.

*Assessing the Impact of Treatment Frequency and Duration on Brain Activation Moderators*

First, we examined whether treatment frequency interacted with any of the brain activation moderators. To do this, we examined the interaction of treatment frequency with the moderator (extracted average beta weights from clusters identified in the voxel-wise moderation analyses) in a three-way interaction model (Time x Treatment Frequency x Moderator) while simultaneously modeling and controlling for all of the lower-order interactions and main effects in an intent-to-treat framework. By necessity, this analysis was conducted only in those individuals randomized to immediate treatment, as individuals randomized to waitlist would not have any assigned value for treatment frequency. These analyses showed that treatment frequency did not interact

with any of the brain activation moderation effects (all *p's* > 0.13), and the brain activation moderators continued to remain significant in the fully specified models.

Next, we examined whether treatment duration moderated brain activation moderators using linear mixed models in an intent-to-treat framework. We modeled this effect as a three-way interaction of Time x Brain Activation Moderator x Treatment Duration while simultaneously controlling for all lower order interactions and main effects (analogous to the analysis for treatment frequency reported above). We observed that treatment duration did not interact with the Time x Brain Activation Moderator (all *p's* > 0.11) across any of the effects reported in the manuscript, and the Time x Brain Activation Moderator effects continued to remain significant in the fully specified models.

*Assessing the Impact of Psychiatric Medication on Brain Activation Moderators*

Finally, to determine whether medication usage might impact the brain moderator results, we excluded the 5 subjects on psychoactive medications and re-ran the brain activation moderation analyses using extracted individual average beta weights for activation from clusters identified in the primary voxelwise analyses. The findings were unchanged, and all moderation effects continued to remain highly significant (all *p's* < 0.01). We also ran an additional set of analyses in which we included the entire sample and specified a variable corresponding to the use of medication (SSRI or benzodiazepine). We then examined this variable in interaction with the moderator (Time x Group x Moderator x Med Use) as well as all lower-order interactions and main effects. Across all analyses, the use of medication did not significantly interact with the

brain activation moderation effect (all *p's* > 0.12). Though these post-hoc analyses are likely underpowered to detect significant interactions of treatment duration, frequency, or medication usage with brain activation moderation effects, they suggest that no large-magnitude interaction effects were clearly present.

*Predictive Value of Brain Moderators for Remission from PTSD*

Comparison Model (Group and Baseline PTSD Symptom Severity)

In order to assess the incremental validity of brain activation moderators in predicting remission from PTSD at the end of the study, a linear discriminant function was first computed using the predictors of group assignment (treatment or waitlist) and baseline PTSD symptom severity (CAPS total score) only. This model provided a canonical discriminant function with an eigenvalue of 0.634 and a canonical correlation of 0.623 (Wilk's lambda = 0.612, $\chi^2$ = 20.138, $p$ < 0.001). This model provided an initial classification accuracy of 81.8% and a leave one out cross-validated accuracy of 79.5% (positive predictive value = 1.00, negative predictive value = 0.74).

Emotional Reactivity Task

Using the effects identified in the *a-priori* region of interest-constrained voxelwise analyses for conscious fear vs. neutral, a linear discriminant function was computed with the predictors of group assignment, baseline PTSD severity, and average activation within each of the 8 identified clusters. This model provided a canonical discriminant function with an eigenvalue of 1.368 and a canonical correlation of 0.760 (Wilk's lambda = 0.422, $\chi^2$ = 31.893, $p$ < 0.001). This model provided an initial

classification accuracy of 90.9% and a leave one out cross-validated accuracy of 84.1% (positive predictive value = 1.00, negative predictive value = 0.79). McNemar's test with an Agresti-Coull correction demonstrated that this model did not provide significantly better classification accuracy relative to the model with only group assignment and baseline severity ($p$ = 0.102).

Using the effects from the whole brain exploratory analysis of the conscious fear vs. neutral contrast, a linear discriminant function was computed with the predictors of group assignment, baseline PTSD severity, and average activation within each of the 15 identified clusters. This model provided a canonical discriminant function with an eigenvalue of 2.658 and a canonical correlation of 0.852 (Wilk's lambda = 0.273, $\chi^2$ = 43.448, $p$ < 0.001). This model provided an initial classification accuracy of 95.5% and a leave one out cross-validated accuracy of 81.8% (positive predictive value = 0.90, negative predictive value = 0.79). McNemar's test with the Agresti-Coull correction demonstrated that this model provided significantly better classification accuracy relative to the model with only group assignment and baseline severity ($p$ = 0.023).

Emotional Conflict Task

Using the effects identified in the *a-priori* region of interest-constrained voxelwise analyses for congruent fear vs. congruent neutral, a linear discriminant function was computed with the predictors of group assignment, baseline PTSD severity, and average activation within each of the 6 identified clusters. This model provided a canonical discriminant function with an eigenvalue of 1.028 and a canonical correlation of 0.712 (Wilk's lambda = 0.493, $\chi^2$ = 26.875, $p$ < 0.001). This model provided an initial

classification accuracy of 93.2% and a leave one out cross-validated accuracy of 84.1% (positive predictive value = 0.9, negative predictive value = 0.82). McNemar's test with an Agresti-Coull correction demonstrated that this model provided significantly better classification accuracy relative to the model with only group assignment and baseline severity ($p$ = 0.041).

Another linear discriminant function was computed using the effect detected in the conflict regulation contrast from the emotional conflict task, along with group assignment and baseline PTSD severity. This model provided a canonical discriminant function with an eigenvalue of 1.408 and a canonical correlation of 0.765 (Wilk's lambda = 0.415, $\chi^2$ = 35.595, $p < 0.001$). This model provided an initial classification accuracy of 93.2% and a leave one out cross-validated accuracy of 90.9% (positive predictive value = 1.00, negative predictive value = 0.88). McNemar's test with an Agresti-Coull correction demonstrated that this model provided significantly better classification accuracy relative to the model with only group assignment and baseline severity ($p$ = 0.041).

Combining Across Tasks

In an effort to determine the best-predicting model, we combined all of the extracted activation values for significant moderation effects across tasks along with group assignment and baseline PTSD severity and computed a stepwise linear discriminant function. This method utilized a minimization of the Wilks lambda as a criterion for model fit, with a criterion for variable entry and removal from the model to be the p-value of the $F$ statistic for each factor (entry: 0.05, removal: 0.10). This model

provided a canonical discriminant function with an eigenvalue of 2.767 and a canonical correlation of 0.857 (Wilk's lambda = 0.265, $\chi^2 = 52.391$, $p < 0.001$). This model provided an initial classification accuracy of 97.7% and a leave one out cross-validated accuracy of 95.5% (positive predictive value = 1.00, negative predictive value = 0.94). McNemar's test with an Agresti-Coull correction demonstrated that this model provided significantly better classification accuracy relative to the model with only group assignment and baseline severity ($p = 0.013$). This model identified the best predictors of PTSD remission identified over 5 steps. Step 1 first included only the ventromedial prefrontal/ventral striatal emotional conflict regulation moderation effect (Wilk's lambda = 0.681, $F = 19.631$, $p < 0.001$). Step 2 added treatment arm (Wilk's lambda = 0.493, $F = 21.117$, $p < 0.001$). Step 3 added the inferior temporal gyrus cluster from the emotional reactivity task (MNI Coordinates -45, -8, -38; Table S2; Wilk's lambda = 0.413, $F = 18.923$, $p < 0.001$). Step 4 added baseline PTSD symptom severity (CAPS total score) to the model (Wilk's lambda = 0.335, $F = 19.384$, $p < 0.001$). The fifth and final step added the left middle frontal gyrus cluster from the whole brain analysis of the emotional reactivity task (MNI Coordinates: -34, 20, 45; Table S2; Wilk's lambda = 0.265, $F = 21.032$, $p < 0.001$).

Limitations

There are several points that should be noted regarding the prediction analyses. First, leave one out cross-validation is not the optimal method for establishing predictive accuracy, as it can result in unstable estimates for prediction error (34). However, we were unable to utilize k-fold cross validation due to the small sample sizes for these

analyses, which by necessity utilize completers only. Second, the predictive accuracy of these models is likely higher than what would be expected in a independent cohort of participants given that the same sample of participants was utilized to train the model and test its predictive accuracy. A more robust test of the predictive model would require an independent cohort of patients as a test sample. Additionally, the regions of interest utilized to define the search space were defined based upon continuous moderation of the difference in symptom change as a function of treatment arm, which shares overlapping variance with the prediction of remission status. Thus, the predictive accuracy estimates should be interpreted with caution and with the knowledge that they are likely overestimates of the true predictive accuracy of brain activation during these paradigms for predicting clinical remission in an independent sample.

*Exploratory Analyses of Brain-Behavior Relationships: Assessing the Functional Significance of Treatment-Moderating Activation*

Emotional Reactivity Task

Using average individual activation values within clusters identified in the region of interest-constrained analysis of the conscious fear vs. neutral contrast of the emotional reactivity task, we observed that across the entire sample at baseline greater activation in the dorsal anterior cingulate/mid-cingulate was associated with lower scores on the DERS Nonacceptance of Emotional Responses subscale (rho = -0.259, $p$ = 0.049). Additionally, greater activation in the right dorsolateral prefrontal cortex (superior/middle frontal gyri; center of mass = 27, 32, 44) was associated with lower scores on the DERS Lack of Emotional Clarity subscale (rho = -0.324, $p$ =

0.013). None of the activation clusters were significantly associated with ERQ subscale scores, and these effects also did not relate to distress ratings during the reappraisal paradigm.

Emotional Conflict Task

We first examined reactivity-related activation for the congruent fear vs. congruent happy contrast. Similar to the emotional reactivity task, greater activation in the dorsal anterior cingulate was associated with lower scores on the DERS Nonacceptance of Emotional Responses subscale (rho = -0.253, $p$ = 0.044). Additionally, greater activation of the right posterior portion of the dorsolateral prefrontal cortex (superior frontal gyrus; center of mass = 23, 2, 69) was associated with lower scores on the DERS Impulse Control Difficulties subscale (rho = -0.322, $p$ = 0.010), as was greater activation in the more anterior portion of the right superior frontal gyrus (BA 9, center of mass = 25, 41, 39; rho = -0.248, $p$ = 0.049).

Next, we examined the conflict regulation effect. Activation in the ventromedial prefrontal cortex/ventral striatum during conflict regulation was not associated with any of the DERS or ERQ subscale scores, but, greater activation in this region at baseline across the entire sample was associated with better behavioral regulation of conflict (rho = -0.364, $p$ = 0.003) as well as less self-reported distress when experiencing the affect from a negative picture during the reappraisal paradigm (Look Negative vs. Look Neutral; rho = -0.321, $p$ = 0.012). Reduction in distress ratings as a function of deliberate regulation of negative

emotion (Reappraise Negative vs. Look Negative) was not associated with activation in this region.

## Supplemental References

1. Fonzo GA, Goodkind MS, Oathes DJ, Zaiko YV, Harvey M, Peng KK, Weiss ME, Thompson AL, Zack SE, Mills-Finnerty CE, Rosenberg BM, Edelstein R, Wright RN, Kole CA, Lindley SE, Arnow BA, Jo B, Gross JJ, Rothbaum BO, Etkin A. Selective effects of psychotherapy on frontopolar cortical function in PTSD. Am J Psychiatry (doi: 10.1176/appi.ajp.2017.16091073).
2. Blake DD, Weathers FW, Nagy LM, Kaloupek DG, Gusman FD, Charney DS, Keane TM. The development of a Clinician-Administered PTSD Scale. Journal of traumatic stress. 1995;8:75-90.
3. First MB, Spitzer RL, Gibbon M, Williams JBW: Structured Clinical Interview for DSM-IV-TR Axis I Disorders, Research Version, Patient Edition (SCID-I/P). New York, Biometrics Research, New York State Psychiatric Institute; 2002.
4. Weathers FW, Ruscio AM, Keane TM. Psychometric properties of nine scoring rules for the clinician-administered Posttraumatic Stress Disorder Scale. Psychological Assessment. 1999;11:124-133.
5. Wechsler D: Wechsler Abbreviated Scale of Intelligence. New York, NY, The Psychological Corporation: Harcourt Brace & Company; 1999.
6. Beck AT, Steer RA, Brown GK. Manual for Beck Depression Inventory-II. 1996.
7. Weathers F, Litz B, Herman D, Huska J, Keane T: The PTSD Checklist (PCL): Reliability, Validity, and Diagnostic Utility. in Annual Convention for the International Society for Traumatic Stresss Studies. San Antonio, TX1993.
8. Skevington SM, Lotfy M, O'Connell KA. The World Health Organization's WHOQOL-BREF quality of life assessment: psychometric properties and results of the international field trial. A report from the WHOQOL group. 2004;13:299-310.
9. Gross JJ, John OP. Individual differences in two emotion regulation processes: Implications for affect, relationships, and well-being. Journal of Personality and Social Psychology. 2003;85:348-362.
10. Gratz KL, Roemer L. Multidimensional Assessment of Emotion Regulation and Dysregulation: Development, Factor Structure, and Initial Validation of the Difficulties in Emotion Regulation Scale. Journal of Psychopathology and Behavioral Assessment. 2004;26:41-54.

11. Etkin A, Klemenhagen KC, Dudman JT, Rogan MT, Hen R, Kandel ER, Hirsch J. Individual differences in trait anxiety predict the response of the basolateral amygdala to unconsciously processed fearful faces. Neuron. 2004;44:1043-1055.
12. Ekman P FW. Pictures of facial affect. . Consulting Psychologists Palo Alto, CA. 1976.
13. Etkin A, Egner T, Peraza DM, Kandel ER, Hirsch J. Resolving emotional conflict: a role for the rostral anterior cingulate cortex in modulating activity in the amygdala. Neuron. 2006;51:871-882.
14. Etkin A, Prater KE, Hoeft F, Menon V, Schatzberg AF. Failure of anterior cingulate activation and connectivity with the amygdala during implicit regulation of emotional processing in generalized anxiety disorder. Am J Psychiatry. 2010;167:545-554.
15. Egner T, Etkin A, Gale S, Hirsch J. Dissociable neural systems resolve conflict from emotional versus nonemotional distracters. Cereb Cortex. 2008;18:1475-1484.
16. Minkel JD, McNealy K, Gianaros PJ, Drabant EM, Gross JJ, Manuck SB, Hariri AR. Sleep quality and neural circuit function supporting emotion regulation. Biology of mood & anxiety disorders. 2012;2:22.
17. Glover GH, Li TQ, Ress D. Image-based method for retrospective correction of physiological motion effects in fMRI: RETROICOR. Magnetic resonance in medicine. 2000;44:162-167.
18. Chen AC, Oathes DJ, Chang C, Bradley T, Zhou ZW, Williams LM, Glover GH, Deisseroth K, Etkin A. Causal interactions between fronto-parietal central executive and default-mode networks in humans. Proc Natl Acad Sci U S A. 2013;110:19944-19949.
19. Berlim MT, Van Den Eynde F. Repetitive transcranial magnetic stimulation over the dorsolateral prefrontal cortex for treating posttraumatic stress disorder: an exploratory meta-analysis of randomized, double-blind and sham-controlled trials. Canadian journal of psychiatry Revue canadienne de psychiatrie. 2014;59:487-496.
20. Boggio PS, Rocha M, Oliveira MO, Fecteau S, Cohen RB, Campanha C, Ferreira-Santos E, Meleiro A, Corchs F, Zaghi S, Pascual-Leone A, Fregni F. Noninvasive brain stimulation with high-frequency and low-intensity repetitive transcranial magnetic stimulation treatment for posttraumatic stress disorder. The Journal of clinical psychiatry. 2010;71:992-999.

21. Foa EB, Hembree EA, Rothbaum BO: Prolonged Exposure Therapy for PTSD. Oxford, Oxford University Press; 2007.
22. Foa EB, Hembree EA, Cahill SP, Rauch SA, Riggs DS, Feeny NC, Yadin E. Randomized trial of prolonged exposure for posttraumatic stress disorder with and without cognitive restructuring: outcome at academic and community clinics. Journal of consulting and clinical psychology. 2005;73:953-964.
23. Jenkinson M, Beckmann CF, Behrens TE, Woolrich MW, Smith SM. FSL. Neuroimage. 2012;62:782-790.
24. Andersson JLR JM, Smith S Non-linear registration, a.k.a. spatial normalisation. FMRIB Technical Report. 2010.
25. Penny W, Friston K, Ashburner J, Kiebel S, Nichols T. Statistical Parametric Mapping: The Analysis of Functional Brain Images. Statistical Parametric Mapping: The Analysis of Functional Brain Images. 2007:1-680.
26. IBM SPSS Statistics for Macintosh, Version 21.0. Armonk, NY, IBM Corp; 2012.
27. Smith SM, Nichols TE. Threshold-free cluster enhancement: addressing problems of smoothing, threshold dependence and localisation in cluster inference. Neuroimage. 2009;44:83-98.
28. Patenaude B, Smith SM, Kennedy DN, Jenkinson M. A Bayesian model of shape and appearance for subcortical brain segmentation. Neuroimage. 2011;56:907-922.
29. Tzourio-Mazoyer N, Landeau B, Papathanassiou D, Crivello F, Etard O, Delcroix N, Mazoyer B, Joliot M. Automated anatomical labeling of activations in SPM using a macroscopic anatomical parcellation of the MNI MRI single-subject brain. Neuroimage. 2002;15:273-289.
30. Kraemer HC, Wilson GT, Fairburn CG, Agras WS. Mediators and moderators of treatment effects in randomized clinical trials. Archives of general psychiatry. 2002;59:877-883.
31. Jose P, Douglas B, Saikat D, Sarkar D, Team. RC: nlme : Linear and Nonlinear Mixed Effects Models. 2015.
32. Team RC: R: A Language and Environment for Statistical Computing. 2015.
33. Agresti A, Coull BA. Approximate is better than "exact" for interval estimation of binomial proportions. The American Statistician. 1998;52:119-126.

34. Shao J. Linear Model Selection by Cross-Validation. Journal of the American Statistical Association. 1993;88:486-494.

**FIGURE S1. Anatomical Regions of Interest Utilized for Voxelwise Analyses**

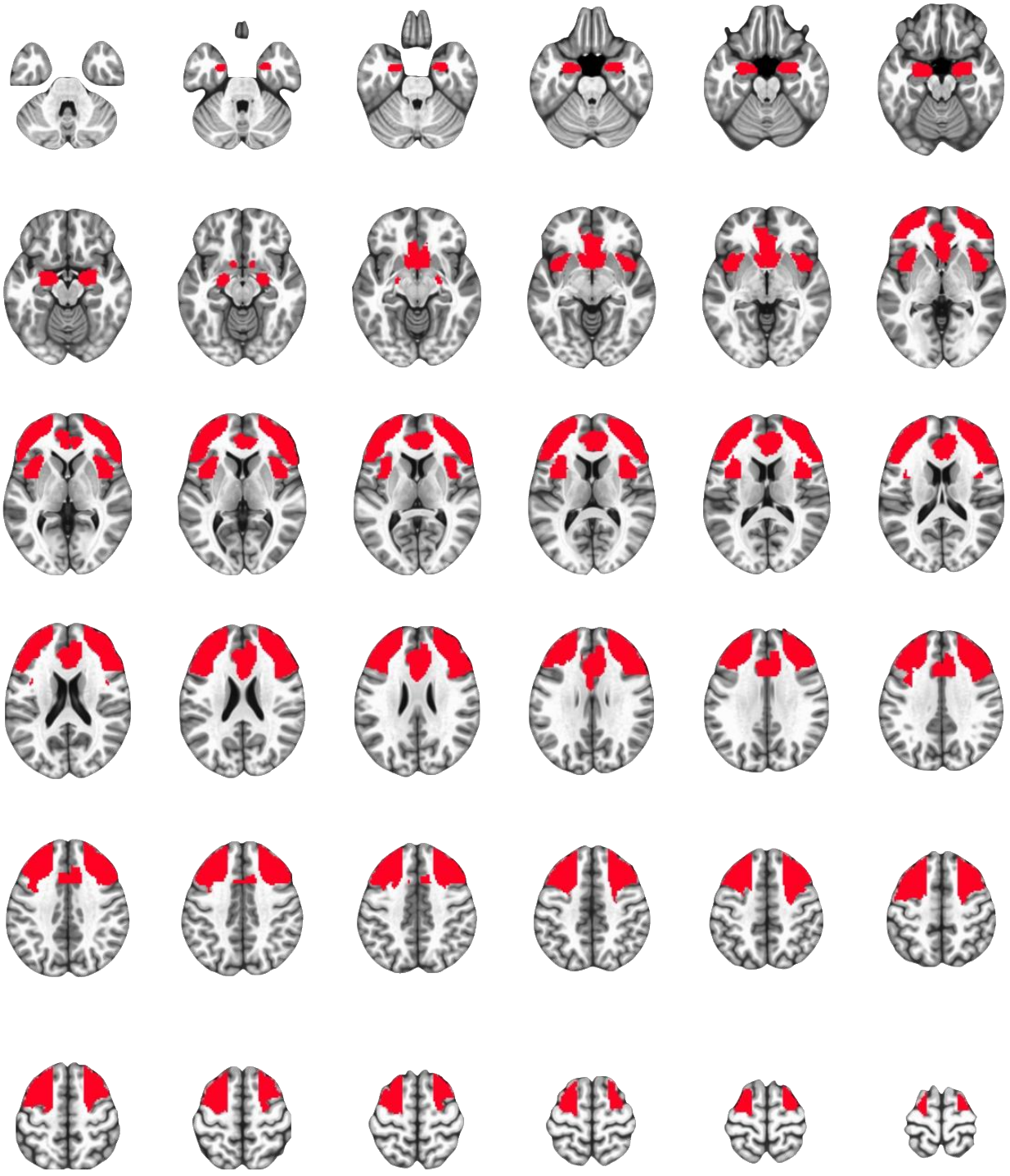

*Figure depicts the anatomical regions of interest utilized for voxelwise analyses overlaid upon the Montreal Neurological Institute average brain with 3mm spacing of slices in the axial plane. Regions of interest included the amygdala, anterior insula, dorsal and ventral anterior cingulate cortex, anterior mid-cingulate cortex, and lateral prefrontal cortex ranging from anterior (frontopolar) to posterior (dorsolateral).*

**FIGURE S2. CONSORT Diagram**

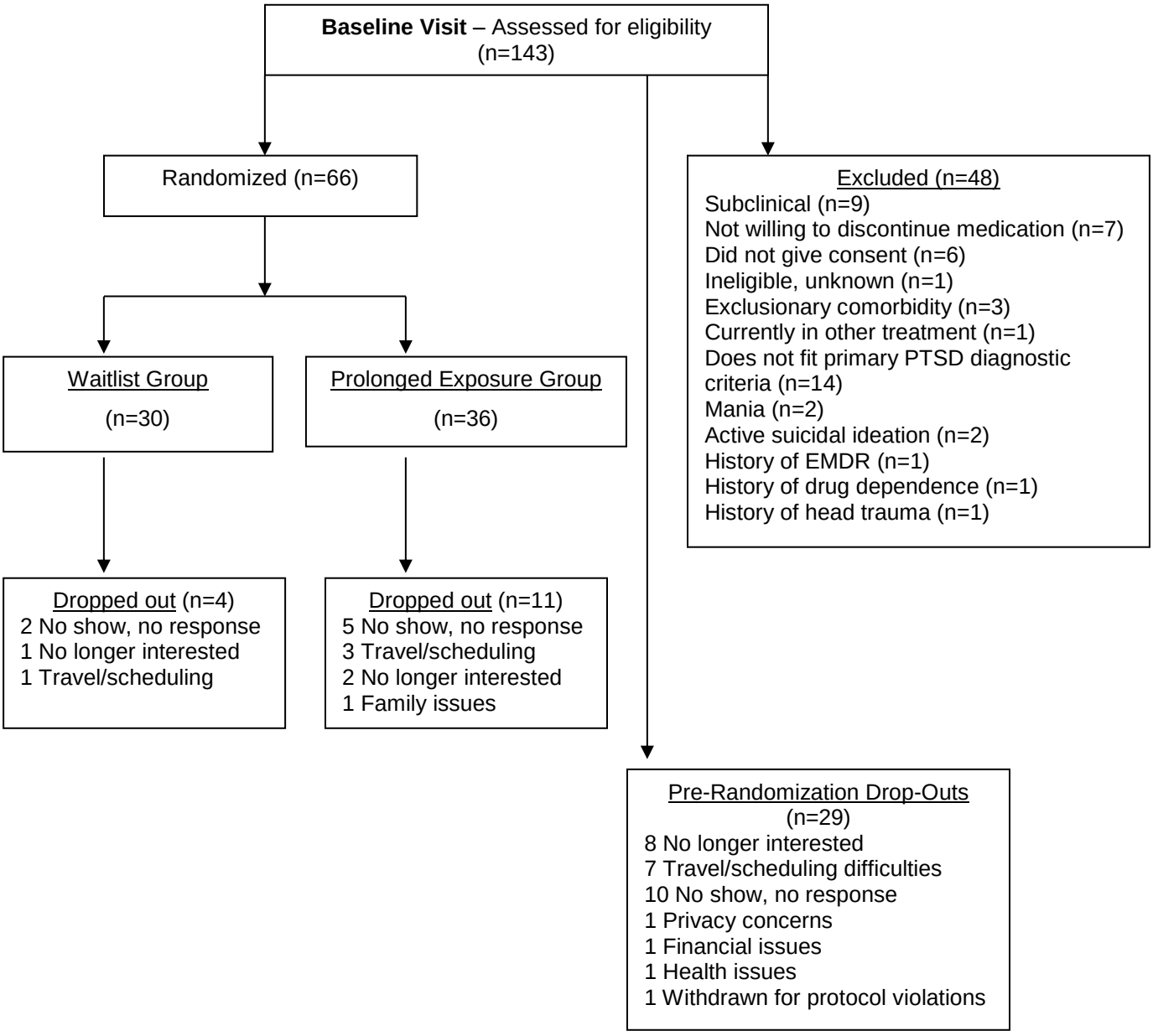

## TABLE S1. Task Dependent Activations/Deactivations At Baseline

| Task | Contrast | Mask | Hem. | MNI Atlas Region(s) | # Voxels | X | Y | Z |
|---|---|---|---|---|---|---|---|---|
| Emo Reac | F-N | ROI | R | Middle Frontal Gyrus/Inferior Frontal Gyrus (P. Triangularis) | 738 | 44 | 21 | 31 |
| Emo Reac | F-N | ROI | R | Insula Lobe | 231 | 38 | 13 | -4 |
| Emo Reac | F-N | ROI | R | Middle Frontal Gyrus | 110 | 27 | 3 | 51 |
| Emo Reac | F-N | ROI | L/R | Middle Cingulate Cortex | 84 | 4 | 16 | 38 |
| Emo Reac | F-N | WB | R | Middle Frontal Gyrus/Inferior Frontal Gyrus (P. Triangularis) | 590 | 44 | 19 | 32 |
| Emo Reac | F-N | WB | R | Superior Parietal Lobule/Precuneus | 568 | 19 | -65 | 59 |
| Emo Reac | F-N | WB | R | Insula Lobe/Temporal Pole | 350 | 45 | 16 | -13 |
| Emo Reac | F-N | WB | L/R | Brainstem | 118 | 0 | -33 | -52 |
| Emo Reac | F-N | WB | R | Middle Frontal Gyrus/Inferior Frontal Gyrus (P. Triangularis) | 32 | 51 | 47 | 5 |
| Emo Reac | F-N | WB | R | Mid-Orbital Gyrus | 23 | 12 | 61 | -4 |
| Emo Reac | MF-MN | ROI | L | Superior Frontal Gyrus | 17 | -26 | 10 | 68 |
| Emo Reac | MF-MN | ROI | R | Middle Frontal Gyrus | 6 | 36 | 24 | 22 |
| Emo Reac | MF-MN | ROI | R | Amygdala | 3 | 24 | -8 | -13 |
| Emo Reac | MF-MN | WB | L/R | Brainstem | 39 | 6 | -21 | -45 |
| Emo Reac | MF-MN | WB | R | Hippocampus (-) | 53 | 24 | -40 | 6 |
| Emo Reac | MF-MN | WB | R | Middle Temporal Gyrus (-) | 27 | 64 | 0 | -22 |
| Emo Reac | MF-MN | WB | R | Putamen | 13 | 20 | 10 | -2 |
| Emo Con | Inc-Con | ROI | L | Insula Lobe | 360 | -36 | 17 | 7 |
| Emo Con | Inc-Con | ROI | R | Insula Lobe | 308 | 39 | 18 | 6 |
| Emo Con | Inc-Con | ROI | L | Superior Frontal Gyrus | 167 | -27 | -5 | 63 |
| Emo Con | Inc-Con | ROI | L | Inferior Frontal Gyrus (P. Triangularis) | 135 | -40 | 20 | 24 |
| Emo Con | Inc-Con | WB | L | Putamen/Insula Lobe/Temporal Pole/Inferior Frontal Gyrus (P. Triangularis/P. Opercularis)/Precentral Gyrus/Middle Frontal Gyrus/Superior Frontal Gyrus/SMA/Middle Cingulate Cortex | 6243 | -24 | 6 | 39 |
| Emo Con | Inc-Con | WB | R | Insula Lobe/Temporal Pole/Inferior Frontal Gyrus (P. Triangularis/P. Opercularis)/Precentral Gyrus/Middle Frontal Gyrus | 2095 | 42 | 15 | 12 |
| Emo Con | Inc-Con | WB | L | Middle Occipital Gyrus/Supramarginal Gyrus/Angular Gyus/Inferior Parietal Lobule/Superior Parietal Lobule | 1813 | -34 | -56 | 41 |
| Emo Con | Inc-Con | WB | L/R | Middle Cingulate Cortex | 493 | 0 | -25 | 30 |

## TABLE S1 (cont). Task Dependent Activations/Deactivations At Baseline

| Task | Contrast | Mask | Hem. | MNI Atlas Region(s) | # Voxels | X | Y | Z |
|---|---|---|---|---|---|---|---|---|
| Emo Con | Inc-Con | WB | L | Middle Temporal Gyrus | 395 | -52 | -53 | 11 |
| Emo Con | Inc-Con | WB | L/R | Midbrain | 206 | -1 | -28 | -12 |
| Emo Con | Inc-Con | WB | R | Precentral Gyrus | 66 | 31 | -15 | 55 |
| Emo Con | Inc-Con | WB | R | Inferior Parietal Lobule | 27 | 34 | -47 | 39 |
| Emo Con | FvH | ROI | L | Inferior Frontal Gyrus (P. Triangularis) | 29 | -40 | 20 | 24 |
| Emo Con | FvH | WB | R | Middle Temporal Gyrus | 17 | 54 | -34 | 4 |
| Emo Con | FvH | WB | L | Hippocampus (-) | 12 | -24 | -18 | -22 |
| Emo Con | iI-cI | ROI | L/R | Anterior Cingulate | 10 | 0 | 36 | 0 |
| Emo Con | iI-cI | ROI | R | Superior Frontal Gyrus/Middle Frontal Gyrus/Inferior Frontal Gyrus (P. Triangularis) (-) | 3232 | 40 | 33 | 23 |
| Emo Con | iI-cI | ROI | L | Superior Frontal Gyrus/Middle Frontal Gyrus/Inferior Frontal Gyrus (P. Triangularis) (-) | 1109 | -37 | 38 | 18 |
| Emo Con | iI-cI | ROI | L/R | Middle Cingulate Cortex (-) | 410 | 5 | 17 | 37 |
| Emo Con | iI-cI | ROI | L | Middle Frontal Gyrus (-) | 167 | -26 | -4 | 58 |
| Emo Con | iI-cI | ROI | R | Insula Lobe (-) | 119 | 33 | 21 | 3 |
| Emo Con | iI-cI | WB | L | Temporal Pole/Inferior Frontal Gyrus (P. Triangularis)/Superior Frontal Gyrus/Middle Frontal Gyrus/Rolandic Operculum/Precentral Gyrus/Anterior Cingulate/Supramarginal Gyrus/Superior Occipital Gyrus/Inferior Parietal Lobule/Superior Parietal Lobule/Postcentral Gyrus/Middle Cingulate Cortex/SMA (-) | 9778 | -25 | -5 | 43 |
| Emo Con | iI-cI | WB | R | Putamen/Insula Lobe/Pallidum/Inferior Frontal Gyrus (P. Triangularis)/Superior Frontal Gyrus/Middle Frontal Gyrus/Precentral Gyrus (-) | 5035 | 39 | 20 | 24 |
| Emo Con | iI-cI | WB | R | Middle Temporal Gyrus/Superior Temporal Gyrus/Middle Occipital Gyrus/Supramarginal Gyrus/Angular Gyrus/Superior Parietal Lobule/Inferior Parietal Lobule/Superior Occipital Gyrus/Postcentral Gyrus/Precuneus (-) | 4070 | 32 | -54 | 46 |
| Emo Con | iI-cI | WB | L | Supramarginal Gyrus (-) | 40 | -57 | -47 | 28 |
| Reap | LNeg-Neut | ROI | R | Middle Frontal Gyrus | 383 | 36 | 10 | 26 |
| Reap | LNeg-Neut | ROI | L | Insula Lobe | 321 | -44 | 16 | 12 |
| Reap | LNeg-Neut | ROI | L | Anterior Cingulate | 314 | -2 | -4 | 30 |
| Reap | LNeg-Neut | ROI | L | Amygdala | 3 | -24 | 2 | -20 |
| Reap | LNeg-Neut | WB | L/R | Cuneus | 996 | -4 | -74 | 20 |
| Reap | LNeg-Neut | WB | L | Middle Occipital Gyrus | 285 | -30 | -90 | -4 |
| Reap | LNeg-Neut | WB | R | Inferior Occipital Gyrus/Fusiform Gyrus | 154 | 36 | -66 | -10 |
| Reap | LNeg-Neut | WB | L | Lingual Gyrus (-) | 190 | -10 | -86 | -2 |

## TABLE S1 (cont). Task Dependent Activations/Deactivations At Baseline

| Task | Contrast | Mask | Hem. | MNI Atlas Region(s) | # Voxels | X | Y | Z |
|---|---|---|---|---|---|---|---|---|
| Reap | LNeg-Neut | WB | L | Postcentral Gyrus (-) | 127 | -46 | -18 | 54 |
| Reap | Reap-LNeg | ROI | R | Middle Frontal Gyrus/Inferior Frontal Gyrus (P. Triangularis/P. Opercularis) | 2579 | 33 | 14 | 43 |
| Reap | Reap-LNeg | ROI | L | Middle Frontal Gyrus/Superior Frontal Gyrus | 540 | -27 | -1 | 55 |
| Reap | Reap-LNeg | ROI | R | Insula Lobe | 216 | 35 | 13 | 0 |
| Reap | Reap-LNeg | WB | L/R | Cerebellum/Cerebellar Vermis/Fusiform Gyrus/Inferior Temporal Gyrus/Lingual Gyrus/Inferior Occipital Gyrus/Middle Occipital Gyrus/Middle Temporal Gyrus/Calcarine Gyrus/Superior Occipital Gyrus/Superior Temporal Gyrus/Cuneus/Supramarginal Gyrus/Precuneus/Postcentral Gyrus/Inferior Parietal Lobule/Angular Gyrus/Superior Parietal Lobule | 26132 | 9 | -69 | 11 |
| Reap | Reap-LNeg | WB | L | Superior Temporal Gyrus/Rolandic Operculum/Postcentral Gyrus/Supramarginal Gyrus/Precentral Gyrus/Inferior Parietal Lobule | 2049 | -44 | -18 | 41 |
| Reap | Reap-LNeg | WB | R | Inferior Frontal Gyrus (P. Opercularis/P. Triangularis)/Middle Frontal Gyrus/Precentral Gyrus | 1965 | 41 | 7 | 37 |
| Reap | Reap-LNeg | WB | L/R | Superior Medial Gyrus/SMA | 361 | 3 | 21 | 49 |
| Reap | Reap-LNeg | WB | L | Superior Parietal Lobule | 125 | -23 | -59 | 49 |
| Reap | Reap-LNeg | WB | R | Precentral Gyrus | 30 | 25 | -13 | 67 |

*X, Y, and Z values are cluster center of mass coordinates in MNI stereotactic space; A negative (-) sign following the MNI Atlas regions indicates that cluster was a deactivation; Task column specifies the functional task from which the cluster was identified, while the contrast column specifies the contrast of task conditions; Emo Con = emotional conflict task; Emo Reac = emotional reactivity task; F-N = conscious (unmasked) fear vs. neutral faces; FvH = congruent fear vs. congruent happy trials; il-cI = conflict regulation (post-incongruent incongruent trials vs. post-congruent incongruent trials); Inc-Con = incongruent vs. congruent trials; L = left; LNeg-Neut = look negative vs. look neutral trials; MF-MN = nonconscious (masked) fear vs. neutral faces; MNI = Montreal Neurological Institute; R = right; Reap = reappraisal task; Reap-LNeg = reappraise negative vs. look negative trials; ROI = region of interest; WB = whole brain.*

## TABLE S2. Treatment Outcome Moderating Activation from Emotional Reactivity Task

| Mask | Hem. | MNI Atlas Region(s) | # Voxels | X | Y | Z | Voxel Stats | | Extractions | | | |
|---|---|---|---|---|---|---|---|---|---|---|---|---|
| | | | | | | | *FDR Z* | | *Parameter, Significance* | | *ROC* | |
| | | | | | | | *Mean* | *SD* | *PE* | *WL* | *Sens* | *Spec* |
| | | Conscious Fear vs. Conscious Neutral | | | | | | | | | | |
| ROI | L | Superior Frontal Gyrus/Middle Frontal Gyrus/Inferior Frontal Gyrus (Pars Triangularis) | 1948 | -31 | 35 | 32 | 2.20 | 0.16 | -43.35, 0.001 | 53.88, 0.001 | 1.00 | 0.80 |
| ROI | L/R | Anterior Cingulate/Middle Cingulate | 727 | 0 | 36 | 25 | 2.21 | 0.16 | -68.30, <0.001 | 14.44, 0.277 | 0.70 | 0.87 |
| ROI | R | Superior Frontal Gyrus/Middle Frontal Gyrus | 627 | 27 | 32 | 44 | 2.26 | 0.18 | -48.73, 0.001 | 45.19, 0.001 | 0.70 | 0.60 |
| ROI | L | Insula Lobe | 156 | -39 | 15 | 6 | 2.15 | 0.14 | -66.11, 0.001 | 21.25, 0.247 | 0.70 | 0.77 |
| ROI | R | Superior Frontal Gyrus/Middle Frontal Gyrus | 116 | 38 | 53 | 12 | 2.23 | 0.17 | -42.39, <0.001 | 5.52, 0.369 | 0.70 | 0.67 |
| ROI | L | Amygdala | 61 | -22 | -7 | -15 | 2.08 | 0.07 | 28.37, 0.012 | -28.21, 0.030 | 0.60 | 0.60 |
| ROI | L | Superior Frontal Gyrus | 56 | -31 | -8 | 66 | 2.16 | 0.14 | -25.61, 0.010 | 8.00, 0.246 | 0.80 | 0.80 |
| ROI | R | Superior Frontal Gyrus | 40 | 23 | 61 | 12 | 2.11 | 0.10 | -24.31, 0.006 | 14.56, 0.035 | 0.60 | 0.87 |
| WB | L | Inferior Temporal Gyrus/Middle Temporal Gyrus | 380 | -61 | -47 | 0 | 2.23 | 0.18 | -37.38, 0.001 | 25.75, 0.009 | 0.60 | 0.71 |
| WB | L | Anterior Cingulate/Middle Cingulate/Superior Medial Gyrus | 357 | -5 | 34 | 35 | 2.15 | 0.16 | -50.66, <0.001 | 34.82, 0.009 | 1.00 | 0.71 |
| WB | L | Inferior Temporal Gyrus | 268 | -45 | -8 | -38 | 2.20 | 0.15 | -49.46, <0.001 | 20.35, 0.042 | 0.90 | 0.93 |
| WB | R | Middle Frontal Gyrus/Superior Frontal Gyrus | 206 | 27 | 34 | 38 | 2.17 | 0.15 | -39.48, 0.001 | 37.36, 0.001 | 0.70 | 0.64 |
| WB | L | Inferior Frontal Gyrus (Pars Triangularis) | 71 | -38 | 19 | 27 | 2.10 | 0.11 | -39.56, 0.003 | 29.38, 0.025 | 0.70 | 0.71 |
| WB | L | Superior Frontal Gyrus | 71 | -19 | 44 | 39 | 2.02 | 0.04 | -29.82, 0.003 | 22.52, 0.009 | 0.70 | 0.78 |
| WB | L | Angular Gyrus | 61 | -44 | -72 | 32 | 2.15 | 0.15 | -32.08, 0.002 | 26.13, 0.016 | 0.80 | 0.65 |
| WB | R | Anterior Cingulate/Middle Cingulate | 60 | 7 | 41 | 28 | 2.07 | 0.10 | -80.17, <0.001 | 15.06, 0.164 | 0.90 | 0.78 |
| WB | L | Middle Frontal Gyrus | 57 | -34 | 20 | 45 | 2.10 | 0.11 | -60.15, <0.001 | 36.29, 0.018 | 0.80 | 0.85 |
| WB | L | Superior Frontal Gyrus | 49 | -23 | 58 | 25 | 2.05 | 0.07 | -31.49, 0.001 | 21.18, 0.005 | 0.90 | 0.93 |
| WB | L | Angular Gyrus/Inferior Parietal Lobule | 41 | -54 | -60 | 37 | 2.08 | 0.09 | -26.08, 0.002 | 15.42, 0.042 | 1.00 | 0.78 |
| WB | L | Inferior Temporal Gyrus | 39 | -63 | -23 | -23 | 2.12 | 0.11 | -35.17, 0.001 | 20.04, 0.058 | 0.70 | 0.85 |
| WB | R | Cerebellum | 36 | 39 | -63 | -37 | 2.12 | 0.14 | -45.31, <0.001 | 19.26, 0.042 | 0.90 | 0.62 |
| WB | L | Middle Temporal Gyrus | 31 | -45 | -76 | 7 | 2.10 | 0.09 | 26.11, 0.003 | -24.80, 0.006 | 0.90 | 0.50 |
| WB | R | Middle Frontal Gyrus | 20 | 38 | 52 | 13 | 2.08 | 0.09 | -44.56, <0.001 | 4.17, 0.467 | 0.70 | 0.64 |

*X, Y, and Z values are cluster center of mass coordinates in MNI stereotactic space; Voxel stats column depicts the mean and standard deviation of the voxelwise statistics for each clustered effect; Extractions column reports the mixed model parameter and significance value using extracted individual cluster beta values for each subject; The ROC column specifies sensitivity and specificity of remission prediction in treatment arm for brain activation in each cluster; FDR = false discovery rate; Hem = hemisphere; L = left; MNI = Montreal Neurological Institute; R = right; ROC = receiver-operator curve; ROI = regions of interest; Sens = sensitivity; Sig. = significance; Spec = specificity; WB = whole brain exploratory analysis.*

## TABLE S3. Treatment Outcome Moderating Activation from Emotional Conflict Task

| Mask | Hem. | MNI Atlas Region(s) | # Voxels | X | Y | Z | Voxel Stats | | Extractions | | | |
|---|---|---|---|---|---|---|---|---|---|---|---|---|
| | | | | | | | *FDR Z* | | *Parameter, Significance* | | *ROC* | |
| | | | | | | | *Mean* | *SD* | *PE* | *WL* | *Sens* | *Spec* |
| | | Congruent Fear vs. Congruent Happy | | | | | | | | | | |
| ROI | R | Middle Frontal Gyrus/Superior Frontal Gyrus | 99 | 29 | 22 | 50 | 1.97 | 0.001 | -8.15, <0.001 | 5.16, 0.013 | 0.60 | 0.80 |
| ROI | R | Superior Frontal Gyrus | 70 | 23 | 2 | 69 | 1.97 | 0.002 | -7.39, <0.001 | 4.09, 0.025 | 0.60 | 1.00 |
| ROI | L | Middle Frontal Gyrus | 58 | -23 | 6 | 65 | 1.97 | 0.001 | -5.70, 0.002 | 4.71, 0.025 | 0.70 | 0.66 |
| ROI | L | Middle Frontal Gyrus | 45 | -32 | 49 | 22 | 1.97 | 0.001 | -5.76, 0.001 | 2.76, 0.020 | 0.70 | 0.53 |
| ROI | R | Superior Frontal Gyrus | 40 | 25 | 41 | 39 | 1.97 | 0.002 | -7.28, <0.001 | 3.31, 0.052 | 0.70 | 0.60 |
| ROI | R | Anterior Cingulate/Middle Cingulate | 13 | 11 | 21 | 30 | 1.97 | 0.001 | -19.85, <0.001 | 5.69, 0.074 | 0.60 | 0.73 |
| | | Post-Incongruent Incongruent vs. Post-Congruent Incongruent (Emotional Conflict Regulation) | | | | | | | | | | |
| ROI | L/R | Olfactory Cortex/Mid-Orbital Gyrus/Anterior Cingulate/Caudate Nucleus | 450 | -3 | 14 | -14 | 2.25 | 0.19 | -26.26, <0.001 | 23.77, 0.006 | 1.00 | 0.79 |
| | | Emotional Conflict Regulation vs. Gender Conflict Regulation | | | | | | | | | | |
| ROI | L/R | Olfactory Cortex/Mid-Orbital Gyrus/Anterior Cingulate/Caudate Nucleus | 218 | -2 | 17 | -7 | 2.28 | 0.21 | -16.68, <0.001 | 5.84, 0.146 | 0.64 | 0.66 |

*X, Y, and Z values are cluster center of mass coordinates in MNI stereotactic space; Voxel stats column depicts the mean and standard deviation of the voxelwise statistics for each clustered effect; Extractions column reports the mixed model parameter and significance value using extracted individual cluster beta values for each subject; The ROC column specifies sensitivity and specificity of remission prediction in treatment arm for brain activation in each cluster; FDR = false discovery rate; Hem = hemisphere; L = left; MNI = Montreal Neurological Institute; R = right; ROI = regions of interest; ROC = receiver-operator curve; Sens = sensitivity; Sig. = significance; Spec = specificity; WB = whole brain exploratory analysis.*

## TABLE S4. Predicted CAPS Total Scores From Linear Mixed Models with Brain Activation Moderators

| Task | Contrast | Mask | Hem. | MNI Atlas Region(s) | X | Y | Z | Predicted CAPS Total Scores | | | | | | | |
|---|---|---|---|---|---|---|---|---|---|---|---|---|---|---|---|
| | | | | | | | | Pre | | | | Post | | | |
| | | | | | | | | PE | | WL | | PE | | WL | |
| | | | | | | | | + | - | + | - | + | - | + | - |
| Emo Reac | F-N | ROI | R | Superior Frontal Gyrus/Middle Frontal Gyrus/Inferior Frontal Gyrus (Pars Triangularis) | -31 | 35 | 32 | 64.8, 6.2 | 69.7, 7.8 | 70.5, 9.8 | 69.0, 8.8 | 19.0, 9.6 | 38.7, 13.2 | 76.5, 11.9 | 57.6, 10.8 |
| Emo Reac | F-N | ROI | L/R | Anterior Cingulate/Middle Cingulate | 0 | 36 | 25 | 66.9, 7.1 | 67.2, 7.7 | 70.4, 11.0 | 68.9,10.4 | 15.6, 12.9 | 39.2, 13.4 | 69.3, 12.2 | 62.2, 11.1 |
| Emo Reac | F-N | ROI | R | Superior Frontal Gyrus/Middle Frontal Gyrus | 27 | 32 | 44 | 67.8, 9.9 | 65.8, 8.1 | 69.0, 11.4 | 70.6, 11.1 | 21.5, 12.1 | 35.5, 14.8 | 74.1, 15.2 | 59.3, 12.1 |
| Emo Reac | F-N | ROI | L | Insula Lobe | -39 | 15 | 6 | 65.4, 6.8 | 68.6, 6.5 | 71.0, 10.3 | 67.8, 9.0 | 16.3, 7.8 | 36.5, 11.8 | 69.4, 12.0 | 60.2, 8.1 |
| Emo Reac | F-N | ROI | R | Superior Frontal Gyrus/Middle Frontal Gyrus | 38 | 53 | 12 | 69.4, 11.0 | 64.7,11.0 | 68.7, 13.2 | 71.7, 11.8 | 19.3, 10.0 | 35.4, 12.1 | 65.8, 14.4 | 65.0, 11.5 |
| Emo Reac | F-N | ROI | L | Amygdala | -22 | -7 | -15 | 64.6, 11.9 | 69.3, 9.9 | 69.4, 11.0 | 70.7, 12.6 | 31.5, 11.3 | 20.8, 7.6 | 59.7, 11.3 | 71.9, 16.7 |
| Emo Reac | F-N | ROI | L | Superior Frontal Gyrus | -31 | -8 | 66 | 64.7, 5.1 | 69.7, 7.1 | 71.8, 9.3 | 66.4, 8.6 | 18.8, 6.8 | 36.7, 11.1 | 70.5, 9.2 | 58.4, 8.4 |
| Emo Reac | F-N | ROI | R | Superior Frontal Gyrus | 23 | 61 | 12 | 69.3, 8.3 | 64.4, 9.9 | 70.2, 12.8 | 69.3, 9.3 | 21.8, 13.6 | 35.4, 13.7 | 71.9, 15.9 | 60.5, 9.0 |
| Emo Reac | F-N | WB | L | Inferior Temporal Gyrus/Middle Temporal Gyrus | -61 | -47 | 0 | 65.9, 4.5 | 69.1, 5.7 | 70.3, 7.1 | 68.2, 7.6 | 16.9, 6.8 | 36.7, 13.6 | 73.6, 12.1 | 57.9, 8.1 |
| Emo Reac | F-N | WB | L | Anterior Cingulate/Middle Cingulate/Superior Medial Gyrus | -5 | 34 | 35 | 64.9, 6.9 | 69.4, 6.2 | 70.4, 10.4 | 68,6, 8.5 | 16.5, 9.6 | 39.1, 13.5 | 73.7, 13.3 | 58.4, 9.9 |
| Emo Reac | F-N | WB | L | Inferior Temporal Gyrus | -45 | -8 | -38 | 64.8, 4.3 | 70.4, 5.9 | 70.0, 8.8 | 68.8, 7.8 | 16.1, 8.2 | 41.0, 10.1 | 69.7, 13.6 | 60.0, 8.3 |
| Emo Reac | F-N | WB | R | Middle Frontal Gyrus/Superior Frontal Gyrus | 27 | 34 | 38 | 67.4, 8.8 | 66.6, 9.3 | 68.7, 10.1 | 70.7, 11.6 | 20.6, 10.4 | 35.4, 15.1 | 72.7, 14.7 | 58.8, 13.0 |
| Emo Reac | F-N | WB | L | Inferior Frontal Gyrus (Pars Triangularis) | -38 | 19 | 27 | 65.7, 5.0 | 68.8, 8.2 | 68.7, 9.0 | 70.1, 9.2 | 19.3, 9.1 | 36.2, 11.7 | 70.1, 14.8 | 60.9, 9.2 |
| Emo Reac | F-N | WB | L | Superior Frontal Gyrus | -19 | 44 | 39 | 65.3, 8.9 | 69.3, 7.8 | 65.9, 9.4 | 72.3, 11.4 | 22.2, 10.8 | 42.0, 14.8 | 68.6, 14.0 | 63.8, 12.5 |
| Emo Reac | F-N | WB | L | Angular Gyrus | -44 | -72 | 32 | 64.7, 6.6 | 70.7, 7.4 | 70.8, 9.9 | 68.9, 9.3 | 17.9, 10.0 | 42.4, 12.9 | 76.4, 11.2 | 59.8, 10.5 |
| Emo Reac | F-N | WB | R | Anterior Cingulate/Middle Cingulate | 7 | 41 | 28 | 66.1, 9.2 | 67.4, 10.0 | 72.3, 12.9 | 67.3, 11.0 | 10.8, 13.3 | 39.8, 14.4 | 71.3, 13.6 | 59.4, 10.5 |
| Emo Reac | F-N | WB | L | Middle Frontal Gyrus | -34 | 20 | 45 | 67.0, 7.6 | 67.6, 8.0 | 73.3, 9.8 | 67.8, 9.3 | 22.9, 10.6 | 39.9, 12.6 | 78.0, 11.9 | 59.4, 10.5 |
| Emo Reac | F-N | WB | L | Superior Frontal Gyrus | -23 | 58 | 25 | 62.6, 6.3 | 72.4, 6.8 | 69.7, 11.8 | 69.9, 9.0 | 17.7, 8.4 | 44.5, 7.1 | 74.3, 12.1 | 59.4, 11.8 |
| Emo Reac | F-N | WB | L | Angular Gyrus/Inferior Parietal Lobule | -54 | -60 | 37 | 65.4, 5.7 | 69.2, 7.3 | 70.3, 8.8 | 68.9, 9.2 | 17.2, 10.6 | 37.6, 13.4 | 72.6, 9.1 | 59.5, 9.5 |
| Emo Reac | F-N | WB | L | Inferior Temporal Gyrus | -63 | -23 | -23 | 65.9, 5.7 | 68.5, 8.4 | 72.3, 9.9 | 67.0, 8.2 | 19.9, 6.8 | 37.1, 12.5 | 71.8, 14.0 | 58.4, 8.7 |
| Emo Reac | F-N | WB | R | Cerebellum | 39 | -63 | -37 | 67.5, 8.1 | 67.0, 7.4 | 72.4, 10.6 | 67.4, 9.1 | 21.2, 9.6 | 40.1, 12.8 | 72.5, 15.1 | 59.1, 9.9 |
| Emo Reac | F-N | WB | L | Middle Temporal Gyrus | -45 | -76 | 7 | 64.2, 9.7 | 70.4, 12.7 | 70.4, 12.1 | 70.0, 12.2 | 32.5, 11.5 | 27.3, 11.7 | 58.3, 13.6 | 69.1, 14.4 |
| Emo Reac | F-N | WB | R | Middle Frontal Gyrus | 38 | 52 | 13 | 69.6, 11.2 | 64.5, 10.7 | 68.9, 13.4 | 71.5, 11.7 | 18.1, 10.3 | 35.9, 13.7 | 65.6, 14.3 | 65.2, 11.6 |

## TABLE S4 (cont). Predicted CAPS Total Scores From Linear Mixed Models with Brain Activation Moderators

| Task | Contrast | Mask | Hem. | MNI Atlas Region(s) | X | Y | Z | Predicted CAPS Total Scores (mean, SD) | | | | | | | |
|---|---|---|---|---|---|---|---|---|---|---|---|---|---|---|---|
| | | | | | | | | Pre | | | | Post | | | |
| | | | | | | | | PE | | WL | | PE | | WL | |
| | | | | | | | | + | - | + | - | + | - | + | - |
| Emo Con | FvH | ROI | R | Middle Frontal Gyrus/Superior Frontal Gyrus | 29 | 22 | 50 | 69.7, 11.3 | 63.9, 6.4 | 69.9, 12.3 | 69.9, 11.0 | 20.5, 17.6 | 37.1, 14.3 | 70.1, 14.0 | 57.5, 12.5 |
| Emo Con | FvH | ROI | R | Superior Frontal Gyrus | 23 | 2 | 69 | 66.1, 7.8 | 68.6, 8.6 | 70.0, 10.2 | 69.6, 11.5 | 14.3, 10.1 | 37.7, 13.0 | 68.1, 12.5 | 56.9, 12.1 |
| Emo Con | FvH | ROI | L | Middle Frontal Gyrus | -23 | 6 | 65 | 68.4, 7.0 | 66.6, 9.9 | 73.2, 8.9 | 66.4, 9.6 | 19.7, 7.5 | 35.1, 12.8 | 71.8, 11.8 | 54.8, 11.9 |
| Emo Con | FvH | ROI | L | Middle Frontal Gyrus | -32 | 49 | 22 | 68.8, 9.8 | 66.2, 8.7 | 73.6, 8.6 | 66.2, 8.7 | 20.1, 12.1 | 34.7, 13.7 | 73.9, 10.3 | 56.1, 12.3 |
| Emo Con | FvH | ROI | R | Superior Frontal Gyrus | 25 | 41 | 39 | 68.3, 10.4 | 66.6, 9.2 | 72.8, 11.8 | 67.8, 11.6 | 18.9, 14.3 | 41.7, 14.8 | 71.2, 11.0 | 57.6, 114 |
| Emo Con | FvH | ROI | R | Anterior Cingulate/Middle Cingulate | 11 | 21 | 30 | 69.3, 10.4 | 66.1, 10.2 | 70.2, 10.1 | 69.7, 13.7 | 17.6, 12.7 | 33.8, 12.8 | 66.7, 12.8 | 59.0, 13.9 |
| Emo Con | iI-cI | ROI | L/R | Olfactory Cortex/Anterior Cingulate/Caudate Nucleus | -3 | 14 | -14 | 67.5, 7.4 | 68.2, 5.6 | 72.0, 9.8 | 67.8, 7.7 | 20.6, 12.8 | 40.1, 10.2 | 75.3, 15.7 | 56.1, 9.4 |
| Emo v Gen | iI-cI | ROI | L/R | Olfactory Cortex/Anterior Cingulate/Caudate Nucleus | -2 | 17 | -7 | 69.8, 5.6 | 65.8, 10.2 | 74.6, 9.9 | 63.9, 7.8 | 21.1, 7.1 | 35.9, 12.6 | 70.4, 11.2 | 53.6, 8.6 |

*X, Y, and Z values are cluster center of mass coordinates in MNI stereotactic space; Predicted CAPS Total Scores columns depict the mean and standard deviation of the predicted CAPS total scores for each activation moderation cluster split by time, group, and moderator value above (+) or below (-) the median; CAPS = Clinician-Administered PTSD Scale; Emo Con = emotional conflict task; Emo Reac = emotional reactivity task; Emo v Gen = emotional conflict vs. gender conflict; F-N = conscious (unmasked) fear vs. neutral faces; FvH = congruent fear vs. congruent happy trials; iI-cI = conflict regulation (post-incongruent incongruent trials vs. post-congruent incongruent trials); L = left; MNI = Montreal Neurological Institute; PE = prolonged exposure group; R = right; ROI = region of interest; SD = standard deviation; WB = whole brain; WL = waitlist group.*